Suppression of Conductance in Surface Superlattices by Temperature and Electric Field

A. Messica, A. Soibel, U. Meirav, Ady Stern, Hadas Shtrikman, V. Umansky, and D. Mahalu

Braun Center for Submicron Research and Department of Condensed Matter Physics, Weizmann Institute of Science, Rehovot 76100, Israel

(Received 22 January 1996; revised manuscript received 1 August 1996)

We present transport measurements on surface superlattices fabricated on a GaAs/AlGaAs two-dimensional electron gas. Significant suppression of the conductance is found with increasing electric fields and with increasing temperature T. We attribute these effects to e-e scattering, which can significantly affect the resistance in the presence of a spatially modulated static potential. [S0031-9007(96)02082-0]

PACS numbers: 73.20.Dx, 73.50.Fq

The concept of a lateral surface superlattice (SSL) dates back almost two decades [1–4]. The idea is to impose a periodic potential on a two-dimensional electron gas (2DEG). This can be achieved, e.g., by a periodic array of surface electrodes, or gates, to which a voltage V_g is applied with respect to the 2DEG. A variety of alternative techniques are known to induce a SSL [5–10]. SSLs are of great experimental interest due to the geometric control and the amplitude tunability of the periodic potential.

Our work was originally motivated by the notion that a periodic potential should induce a spectrum of Bloch minibands and minigaps, which depends on the gate geometry and on V_g. Furthermore, because of their low scattering rates, SSLs should offer a favorable testing ground to study Wannier-Stark (WS) localization and Bloch oscillations in the presence of longitudinal electric fields [3]. The observation of minigaps in the electronic spectrum of SSLs via transport has long been an important, yet elusive, goal. Indeed, there have been several early reports of nonmonotonic dependence of the resistance on V_g, which were interpreted as resulting from the Fermi energy, E_F sweeping through the miniband spectrum [11–13]. Unfortunately, these results have been difficult to reproduce, despite subsequent improvement in fabrication technology and sample quality. On the other hand, the presence of the periodic potential in the 2DEG leads to distinct features in the magnetoresistance of SSLs [5–7,14].

In this paper we report the results of transport measurements in various SSL devices. We study the dependence of the current I on the drain-source voltage V_{ds}, on the gate voltage V_g and on temperature T. We find a rapid drop in the differential conductance $G \equiv dI/dV_{ds}$ as we increase V_{ds}. We also find a significant decrease in conductance as T is increased in the range of 2–10 K. We interpret these results in terms of electron-electron (e-e) scattering in the presence of the modulated gate potential.

The samples were fabricated on high mobility 2DEGs formed by GaAs/AlGaAs heterojunctions, with Schottky gate electrodes patterned via electron beam lithography. The SSLs had a period $a = 100$, 200, or 300 nm. We have studied devices of several different wafers and geometries, including short gratings as well as long Hall bars covered entirely by a grating gate. Figure 1 shows a short grating sample. We also had control samples, which were Hall bars covered with a single uniform gate but otherwise identical geometry. In all measurements the current flows along the direction of potential modulation, i.e., transverse to the grating lines. Our magnetoresistance

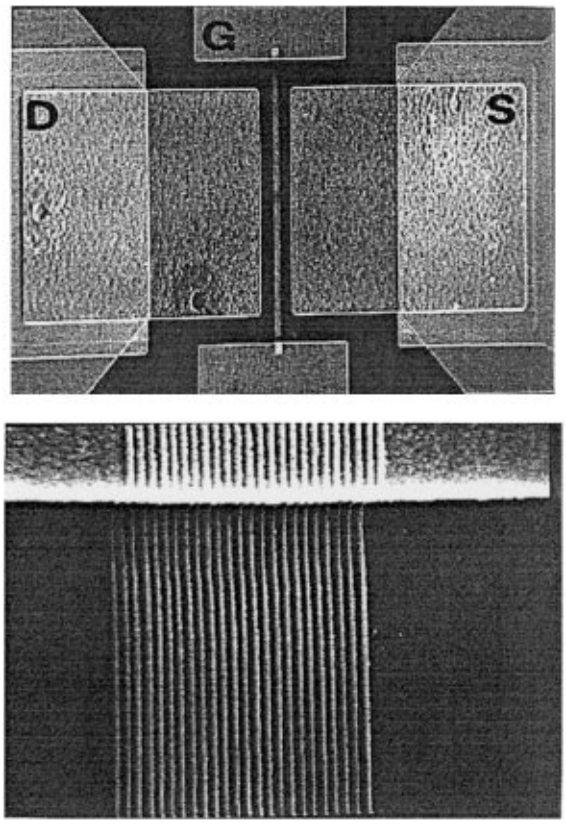

FIG. 1. Scanning electron micrograph of a short SSL sample, consisting of a high mobility 2DEG with a grating gate of 25 metallic wires. The period in the above sample is 100 nm. Top: lower resolution picture, showing the Ohmic contacts D and S (large, brighter shade areas) at both ends of the SSL, and the 2.5×60 μm gate array in the middle. Bottom: the gate wires seen at higher magnification, including their connection to the gate contact pad, G. Current flows in the underlying 2DEG in the direction crossing the gate wires.

measurements (not shown) verified the presence and the strength of the periodic potential [5–7].

Sweeping V_g gave rise to a smooth change in the low-bias conductance, usually with no noteworthy features; on occasion, we found sample-dependent features in the conductance, which could not sensibly be associated with superlattice minibands and minigaps. The discussion of this "negative" result will be the subject of a separate publication.

However, our interest was aroused by the behavior observed in the measurements of G vs V_{ds}. This is shown in Fig. 2 for a sample with $a = 200$ nm, length $L = 5$ μm, and mobility 2.5×10^6 cm^2/V s. The plot shows G vs V_{ds} for a variety of gate voltages, measured at $T = 1.5$ K. With $V_g = 0$ (trace A), we find essentially linear behavior, namely, $G \approx$ const. As the modulated potential is strengthened by increasing $|V_g|$, in addition to the overall decrease of G, a negative slope of G vs $|V_{ds}|$ develops; in other words, the conductance has a peak at zero bias and is suppressed by a longitudinal electric field $F \approx V_{ds}/L$. The suppression of G is observable for V_{ds} as low as 1 mV, corresponding to $F \sim 2$ V/cm. We also measured the dependence of G on temperature in these devices, and found that it decreases rapidly as T is increased in the range of 2–10 K. In fact, we found that the resistance $1/G$ increases quadratically with T.

This observation led us to perform a systematic study of the temperature dependence in SSLs with Hall bar geometry. We remark that the short devices discussed above are optimized for I vs V_{ds} measurements, but they introduce a complication associated with the inevitable transition between the 2DEG outside the gate and the part under the gate. (In fact, some of the features we observe in the short SSLs may be influenced by this transition, as well as by the intrinsic properties of the SSL). In contrast, a Hall bar geometry allows true four-terminal measurement of the low-bias sheet resistance, ρ, and also the determination of the 2DEG density, n, by the Shubnikov–de Haas effect. We now discuss the results on these structures.

In Fig. 3(a) we plot $(\Delta\rho)/\rho$ vs temperature for a SSL with $a = 300$ nm. Here $\Delta\rho$ denotes the change in resistance with respect to its lowest T value. We see large nonlinear increase in the resistance with T, which is enhanced by increasing $|V_g|$. In order to single out the role of the SSL potential from the effects of phonons and disorder, we show in Fig. 3(b) the behavior of a sample (on the same chip) with the same geometry but with a single uniform gate, as described before. While here, too, there is an increase in ρ with temperature, which we attribute to acoustic phonon scattering [15,16], not only is it up to an order of magnitude weaker (for large gate bias), but there are two qualitative differences apparent in the figure. First, in the SSL, the T dependence becomes stronger with increasing gate voltage, while the *opposite* trend is seen in the uniform-gate device, where

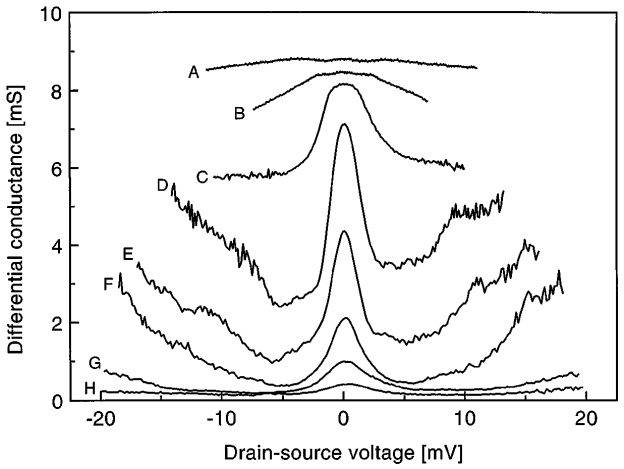

FIG. 2. Differential conductance G vs V_{ds} in a 25-period SSL with $a = 200$ nm, for several fixed values of V_g, as follows: (A) 0 V, (B) −0.15 V, (C) −0.2 V, (D) −0.25 V, (E) −0.3 V, (F) −0.35 V, (G) −0.4 V, and (H) −0.45 V. The measurements were made at $T = 1.5$ K. The curves exhibit a peak at zero bias and a decline in G as the drain-source field is increased. This feature, absent at $V_g = 0$ (A), evolves gradually with V_g, and is associated with the induced gate potential, as discussed in the text.

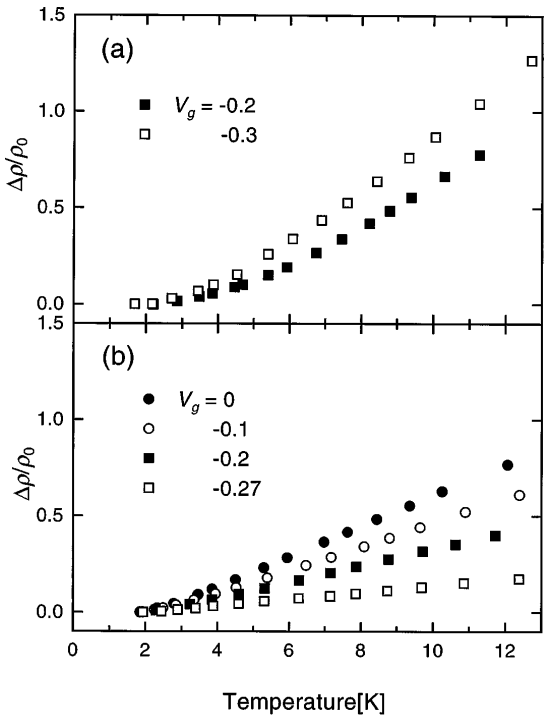

FIG. 3. Temperature dependence of the sheet resistance (a) in a SSL with $a = 300$ nm, and (b) in a 2DEG with a single uniform gate. The quantity plotted, $\Delta\rho/\rho_0$, is the change in resistance normalized to its low temperature value. Note how in (a) the T dependence is nonlinear and becomes stronger with increasing gate potential, while in (b) it is linear and becomes less steep with increasing $|V_g|$. In (b) we are merely seeing the effect of acoustic phonons, while in (a) we observe a unique SSL effect, which we attribute to e-e scattering.

the relative importance of phonons decreases as the 2DEG is depleted and the mobility decreases. Second, the SSL shows apparently quadratic T dependence, while in the uniform device the dependence is approximately linear in most of the range studied.

It is natural to try to understand this T dependence in terms of an increase in the scattering rate. But, in order to explain the experimental observations, the scattering mechanism responsible for this increase has to be quadratically T dependent and to be sensitive to the presence of a modulated external potential. We suggest that this mechanism is e-e scattering. It is well known that e-e scattering does not contribute to the resistance in a translationally invariant system, but can do so in the presence of a modulated external potential [17,18].

Although any removal of translational invariance—not necessarily a periodic one—can lead to a resistive effect from e-e scattering, we will restrict our analysis to the particular case of a periodic potential, since this is the case at hand. Here, as is well known, the electronic spectrum forms a sequence of minibands and minigaps within a mini-Brillouin zone of $\pm\pi/a$.

In an electron-electron scattering event, two electrons of momenta $\boldsymbol{k}_i$, miniband indices l_i, energies $\epsilon_i = \epsilon(l_i, \boldsymbol{k}_i)$, and velocities $\boldsymbol{v}_i = (1/\hbar)\nabla_k \epsilon(l_i, \boldsymbol{k}_i)$, where $i = 1$ and 2, are scattered to momentum states $\boldsymbol{k}_1 + \boldsymbol{q}$, $\boldsymbol{k}_2 - \boldsymbol{q}$ with band indices, energies, and velocities denoted by primes, respectively. The resulting change in current j_x is proportional to the net change in the velocity, $\Delta v_x \equiv (\boldsymbol{v}_1' + \boldsymbol{v}_2' - \boldsymbol{v}_1 - \boldsymbol{v}_2)_x$. There are two quantities of interest for our discussion: One is the e-e scattering rate $\tau_{e\text{-}e}^{-1}$, averaged over all states within kT of the Fermi surface, and the second is the contribution of this process to the resistance, $\rho_{e\text{-}e}$. The former is given by

$$\tau_{e\text{-}e}^{-1} = \frac{8\pi}{\hbar}\frac{E_F}{nkT}\sum_{\substack{k_1,k_2,q\\ l_1,l_2,l_1',l_2'}} |U_q|^2 \times \Phi \times \delta(\Delta\epsilon), \qquad (1)$$

while $\rho_{e\text{-}e}$ has the form [19]

$$\rho_{e\text{-}e} = \frac{2\pi m^2}{\hbar e^2 n^2 kT}\sum_{\substack{k_1,k_2,q\\ l_1,l_2,l_1',l_2'}} |U_q|^2 \times \Phi \times \delta(\Delta\epsilon) \times (\Delta v_x)^2. \qquad (2)$$

In Eqs. (1) and (2), $\Phi = f_1 f_2 (1 - f_1')(1 - f_2')$, where f_i is the Fermi-Dirac distribution function for energy ϵ_i, U_q is the matrix element of the Coulomb interaction, and $\Delta\epsilon \equiv \epsilon_1 + \epsilon_2 - \epsilon_1' - \epsilon_2'$. In the absence of an external potential we have $\boldsymbol{v}(\boldsymbol{k}) \propto \boldsymbol{k}$; hence $\Delta v_x = 0$, and, although the scattering rate (1) is finite, the contribution to the resistance (2) vanishes. However, this is not the case in the presence of a periodic potential, where the energy and velocity are a nontrivial function of $\boldsymbol{k}$.

Using Mathiessen's rule, the total resistance ρ is the sum of the e-e contribution $\rho_{e\text{-}e}$, the phonon contribution $\rho_{\rm ph}$, and the T-independent resistance $\rho_{\rm imp}$ due to impurity scattering:

$$\rho(T) = \rho_{\rm imp} + \rho_{\rm ph}(T) + \rho_{e\text{-}e}(T). \qquad (3)$$

In our measurements, the uniform gate devices shown in Fig. 3(b) correspond to the case of no periodic potential, and the observed T dependence of ρ is entirely due to phonons. This dependence is known to be linear in T for temperatures above a few K [15,16], and our results for these samples are in *quantitative* agreement with the literature.

Equations (1) and (2) both have a characteristic behavior at low T, with the leading terms proportional to T^2 and $T^2\ln(T)$ [20–22]. In fact, there is a simple low-T expansion for (1) in a 2DEG,

$$\tau_{e\text{-}e}^{-1} = \gamma(kT)^2/2\pi\hbar E_{\rm F}[1 + \ln(2q_{\rm TF}/k_{\rm F}) - \ln(kT/E_{\rm F})], \qquad (4)$$

where γ is a prefactor of order unity, whose value is debated in the literature [22–24] and given, e.g., in [22] by 1, while in [24] it is $(\pi/2)^2$. Here $q_{\rm TF} \approx 2 \times 10^6$ cm^{-1} is the Thomas-Fermi wave vector in the 2DEG.

As for the resistance, the above implies that e-e scattering in the presence of a modulated potential should give rise to a term $\rho_{e\text{-}e}$ which, at low temperature, is approximately quadratic in T with a possible logarithmic correction [19]. This could be checked simply by plotting ρ vs T^2; however, we can perform a more quantitative evaluation as follows. Consider the limit where $\Delta v_x \sim v_{\rm F}$, the latter being the Fermi velocity. In this case Eqs. (1) and (2) are simply related by $\rho_{e\text{-}e} \sim (m/ne^2)\tau_{e\text{-}e}^{-1}$, i.e., the Drude form. Generally, we can write $\rho_{e\text{-}e} = \alpha(m/ne^2)\tau_{e\text{-}e}^{-1}$, where $\alpha(<1)$ describes the effectiveness of the periodic potential in converting e-e scattering into resistance.

In order to test this model we define the *experimental* quantity $\tau_{\rm SSL}^{-1}$, obtained by subtracting from $\rho(T)$ the impurity part $\rho_{\rm imp} \equiv \rho(T \approx 0)$ and the known $\rho_{\rm ph}(T)$, which is linear in T, and multiplying by ne^2/m. This definition is motivated by the Drude formula above, with $\tau_{\rm SSL}^{-1} = \alpha\tau_{e\text{-}e}^{-1}$. The procedure is a reasonable approximation for $T > 4$ K, where $\rho_{\rm ph}(T)$ is quite linear. In Fig. 4 we plot $\tau_{\rm SSL}^{-1}$ vs T^2 for several gate voltages. The T dependence appears quadratic; deviation from quadratic behavior could be due to the logarithmic correction, although the available temperature range is insufficient to validate this. For $V_{\rm g} = -0.3$ V, we have $n \approx 1 \times 10^{11}$ cm^{-2}, which yields $\tau_{e\text{-}e}^{-1} \approx 0.5\gamma T^2 \times \{6 - \ln(T)\} \times 10^9$ sec^{-1} K^{-2}, with T in kelvin. The experimental slope of $\tau_{\rm SSL}^{-1}$ vs T^2 (Fig. 4) for this $V_{\rm g}$ is very close to 2×10^9 sec^{-1} K^{-2}; in other words α smaller than (but comparable to) 1. For weaker $V_{\rm g}$ the value of α is much smaller. While many qualifications apply to this quantitative comparison, the agreement is encouraging and supports the idea that the observations can be attributed to e-e scattering, whose

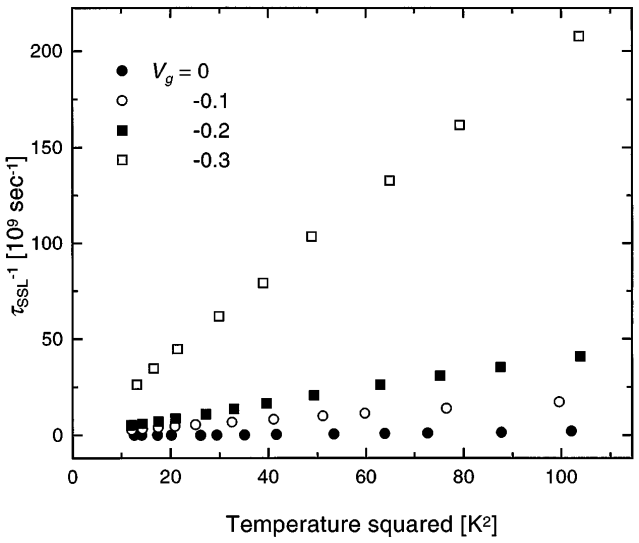

FIG. 4. The quantity τ_{SSL}^{-1}, described in the text, plotted versus T^2. The approximate quadratic dependence suggests that this is a manifestation of *e-e* scattering, while the slope is proportional to the parameter α, which measures the effectiveness of the SSL potential in converting *e-e* scattering into resistance. Note how α vanishes for $V_{\mathrm{g}} = 0$ and increases as the periodic potential is strengthened.

effectiveness in generating resistance (α) increases as the SSL potential is strengthened.

Furthermore, *e-e* scattering could also explain the suppression of G with electric field (Fig. 2), which we observe at low T and larger V_{ds}. An electron accelerated above a cold Fermi sea is susceptible to *e-e* scattering whose energy dependence is similar to the T dependence of *e-e* scattering for the case of thermal electrons at finite T [20–22]. The same consideration holds regarding the role of the periodic potential in translating this scattering into a resistance. Under high fields, if the *e-e* scattering rate exceeds that of other energy loss mechanisms, it will involve heating of the entire electron system [25]. In this sense there is an intimate connection between increasing electric field and increasing temperature.

Finally, we return to the question of minibands. Our experimental results clearly show that a modulated potential is playing a key role in generating resistance from *e-e* scattering, and we have a quantum mechanical formulation of this mechanism in terms of a nonparabolic energy dispersion. However, so far at least, the results fall short of actually evidencing a superlattice band structure with minigaps.

In conclusion, transport in surface superlattice devices shows nonlinearity and a strong quadratic temperature dependence. We have discussed how *e-e* scattering, in the presence of a modulated potential, can contribute to the resistance at finite temperatures or at finite electric fields. In this sense, surface superlattices provide a remarkably clear signature of *e-e* scattering.

We would like to thank E. Gornik, M. Heiblum, Y. Levinson, B. Laikhtman, R. Landauer, and D. Prober for useful discussions. A.M. acknowledges the support of the Israeli Ministry of Science and the S. & R. Benin Foundation. This work was supported by the MINERVA Fund and by The Israel Science Foundation administered by the Israeli Academy of Science and Humanities.

[1] H. Sakaki, K. Wagatsuma, J. Hamasaki, and S. Saito, Thin Solid Films **36**, 497 (1976).
[2] R. T. Bate, Am. Phys. Soc. **22**, 407 (1977).
[3] R. K. Reich, D. K. Ferry, R. O. Grondin, and G. J. Iafrate, Phys. Lett. **91A**, 28 (1982).
[4] J. P. Kotthaus and D. Heitmann, Surf. Sci. **113**, 481 (1982).
[5] D. Weiss, K. von Klitzing, K. Ploog, and G. Weimann, Europhys. Lett. **8**, 179 (1989).
[6] R. W. Winkler, J. P. Kotthaus, and K. Ploog, Phys. Rev. Lett. **62**, 1177 (1989).
[7] E. S. Alves, P. H. Beton, M. Henini, L. Eaves, P. C. Main, O. H. Hughes, G. A. Toombs, S. P. Beaumont, and C. D. W. Wilkinson, J. Phys. Condens. Matter **1**, 8257 (1989).
[8] H. L. Stormer, L. N. Pfeiffer, K. W. Baldwin, K. W. West, and J. Spector, Appl. Phys. Lett. **58**, 726 (1991).
[9] J. Smoliner, V. Rosskopf, G. Berthold, E. Gornik, G. Bohm, and G. Weimann, Phys. Rev. B **45**, 1915 (1992).
[10] M. Krishnamurthy, A. Lorke, M. Wassermeier, D. R. M. Williams, and P. M. Petroff, J. Vac. Sci. Technol. B **11**, 1384 (1993).
[11] A. C. Warren, H. I. Smith, D. A. Antoniadis, and J. Melngailis, IEEE Electron Device Lett. **6**, 294 (1985).
[12] K. Ismail, W. Chu, D. A. Antoniadis, and H. I. Smith, Appl. Phys. Lett. **52**, 1071 (1988).
[13] C. G. Smith, *et al.*, J. Phys. Condens. Matter **2**, 3405 (1990).
[14] C. W. J. Beenakker, Phys. Rev. Lett. **62**, 2020 (1989).
[15] P. J. Price, Surf. Sci. **113**, 199 (1982).
[16] V. Karpus, Sov. Phys. Semicond. **21**, 1180 (1987).
[17] J. M. Ziman, *Electrons and Phonons* (Clarendon Press, Oxford, 1960).
[18] V. F. Gantmakher and Y. B. Levinson, *Carrier Scattering in Metals and Semiconductors* (North-Holland, Amsterdam, 1987).
[19] O. Entin-Wohlman and Y. Imry, Phys. Rev. B **45**, 1590 (1992).
[20] C. Hodges, H. Smith, and J. W. Wilkins, Phys. Rev. B **4**, 302 (1971).
[21] A. V. Chaplik, Sov. Phys. JETP **33**, 997 (1971).
[22] G. F. Giuliani and J. J. Quinn, Phys. Rev. B **26**, 4421 (1982).
[23] A. Yacoby, PhD thesis, The Weizmann Institute, 1994.
[24] L. I. Zheng and S. Dassarma, Phys. Rev. B **53**, 9964 (1996).
[25] C. Wirner, C. Kiener, W. Boxleitner, M. Witzany, E. Gornik, P. Vogl, G. Bohm, and G. Weimann, Phys. Rev. Lett. **70**, 2609 (1993).